Electronic Supplementary Material (ESI) for Nanoscale.
This journal is © The Royal Society of Chemistry 2015

Supplementary information

Design of Magnetic Molecularly Imprinted Polymer Nanoparticles for Controlled Release of Doxorubicin under Alternative Magnetic Field in Athermal Conditions.

N. Griffete [a,*], J. Fresnais[a], A. Espinosa[b], C. Wilhelm[b], A. Bée[a], C. Ménager[a].

Dr. N. Griffete, Dr. J. Fresnais, Dr. A. Bée and Prof. C. Ménager
Sorbonne Universités, UPMC Univ Paris 06, CNRS, Laboratoire PHENIX, Case 51, 4 place Jussieu, F-75005 Paris, France
Email: nebewia.griffete@upmc.fr
Dr. A. Espinosa, Dr. C. Wilhelm
MSC, UMR CNRS 7057, University Paris Diderot, 75205 Paris cedex 13, France.

Materials

Acetonitrile (99.8%), ethanol (99.8%), hydrochloric acid (37%), nitric acid (52%), iron (III) nitrate nonahydrate ($Fe(NO_3)_3$ $9H_2O$, 99%), iron(III) chloridehexahydrate ($FeCl_3.6H_2O$, 97%), acetone, ether, acrylic acid, ethylene glycol dimethylacrylate (EGDMA), Acrylamide, doxorubicin (DOX) from Sigma-Aldrich were used as received. Iron(II) chloride tetrahydrate ($FeCl_2.4H_2O$, 98%) Azo bis isobutyronirile (AIBN), ammonia (20%) were purchased from Acros.

Instrumentation

Transmission Electron Microscopy (TEM). Fe_2O_3 NPs and Fe_2O_3@DOX-MIP NPs were observed using a Jeol-100 CX TEM. A droplet of diluted nanoparticles suspension in water was deposited on a carbon coated copper grid and the excess was drained using filter paper. Size analysis was achieved on TEM images using ImageJ software.

Dynamic light scattering (DLS). Hydrodynamic diameter (d_h) measurements (Malvern Instruments Nanosizer) were recorded starting from pH 2 until to pH 11 by addition of NaOH

with an equilibration time of one minute at each point. The measurements were repeated twice.

Zeta potential. Zeta potential measurements (Malvern Instruments Nanosizer) were recorded starting from pH 2 to pH 11 by addition of NaOH with an equilibration time of one minute for each point. The measurements were repeated twice.

Fourier Transform Infra-Red (FT-IR.) FT-IR spectra of Fe_2O_3 NPs and Fe_2O_3@DOX-MIP NPs were recorded on a Bruker Tensor 27 spectrometer on pressed KBr pellets. Spectra were obtained at regular time intervals in the MIR region of 4000 – 400 cm^{-1} at a resolution of 4 cm^{-1} and analyzed using OPUS software.

Hyperthermia experiments. Hyperthermia experiments for nanoparticles in suspension were conducted on a magneTherm apparatus (magneTherm AC system, Nanotherics Corp) at 335 kHz and 9mT. The sample was heated at 37°C before the application of the alternative magnetic field. The temperature was probed using a fluorooptic fiber thermometer.

For the cell study, we used a home-made magnetothermal setup consisting of a resonant RLC circuit connected to a copper coil in which the temperature was kept constant at 37 ºC. The measurements were performed at 700 kHz and 25 mT.

Ultraviolet-visible spectrophotometry (UV-vis). Absorbance measurements were done with an Avantes UV-visible spectrophotometer, with 100 µm optical fibers. UV/VIS measurements were configured with a range from 200 to 1100 nm. A combined deuterium-halogen light source was used.

Iron Titration. The total iron concentration (M) was determined by atomic absorption spectroscopy (AAS) with a Perkin-Elmer Analyst 100 apparatus after degradation of Fe_2O_3 NPs in boiling HCl (35%).

Synthesis

Synthesis of γ-Fe_2O_3 NPs. Maghemite nanoparticles (γ-Fe_2O_3) were obtained by coprecipitation of Fe^{3+} and Fe^{2+} ions according to Massart's procedure. Magnetite (Fe_3O_4) nanocrystals were prepared by coprecipitation of $FeCl_3$ (1.6 mol) and $FeCl_2$•$4H_2O$ (0.9 mol) salts in alkaline solution (NH_4OH, 7 mol). The solid phase was separated from the supernatant by magnetic separation and immersed in a boiling solution (100°C) of ferric nitrate ($Fe(NO_3)_3$, 0.8 mol) during 30 minutes to completely oxidize magnetite into maghemite (γ-Fe_2O_3). After magnetic decantation, 2 L of distilled water and 360 mL of HNO_3 20% were added to the solution and the mixture was stirred for 10 min. After washing steps in acetone and diethyl-ether to remove the excess of ions, as prepared maghemite nanoparticles were suspended in water. The volume fraction and average size of the maghemite grains were determined by fitting the magnetization curve using Langevin's law. The magnetic size of the particles was also determined by TEM. The final iron content was checked by AAS (C_{Fe} = 1.1 M) after degradation of the nanoparticles in acidic media (boiling HCl 35%).

Surface Modification. The surface of γ-Fe_2O_3 NPs was modified with acrylic functions by the following procedure. 5 mL of the suspension ([Fe] = 1 M) was added to 15 mL of ethanol under ultrasonication, followed by the addition of 20 µL of acrylic acid. The mixture was shaken at a rate of 300 rpm for 2 h. The acrylic acid monomers were anchored at the surface of Fe_2O_3 by complexation with unsaturated iron ions at the nanoparticle surface. The final product of Fe_2O_3-AA was separated and purified by magnetic collection and washed with ethanol and deionized water for three time. The existence of acrylic acid at the surface of Fe_2O_3 NPs was evidenced by the Fourier transform infrared (FT-IR) spectroscopy.

Molecular Imprinting of Doxorubicin at the surface of Fe_2O_3 NPs (Fe_2O_3@DOX-MIP). Acrylamide and EGDMA were used as the functional monomer and cross-linking agent of the imprinting polymerization respectively. 5 mL of the suspension containing Fe_2O_3-AA NPs ([Fe] = 0.2 M) was dispersed in 60 mL of acetonitrile by ultrasonication. Samples of 8 mg of acrylamide (0.1 mmol), 85 µL of EGDMA (0.45 mmol), 2.2 mg of Doxorubicin (0.004 mmol)

as the template, and 5 mg of AIBN (0.03 mmol) as the polymerization initiator were then mixed into the suspension. The mixture was purged with nitrogen for 20 min and then the polymerization could proceed by increasing the temperature at 70 °C for 16 h. The final product consisting of Fe_2O_3@DOX-MIP NPs was dialyzed during 24 hours with a membrane of 6000 g mol^{-1} MWCO, washed several times by magnetic separation and finally dispersed in water. Fe_2O_3@RHO-MIP (for rhodamine) and Fe_2O_3@FLUO-MIP (for fluorescein) nanoparticles were synthesized by using the same procedure with a different weight mass (1.4 mg for FLUO and 2 mg for RHO).

Nanoparticles characterization

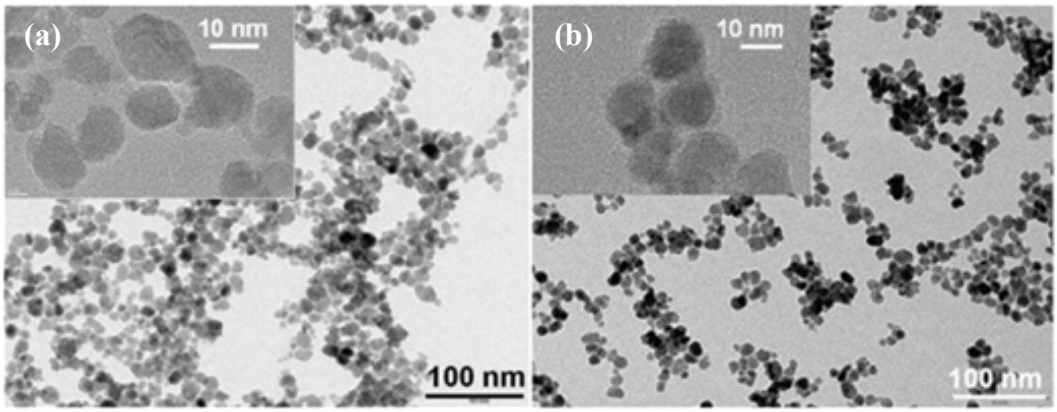

Figure S1. TEM images and high resolution TEM images (inset) of bare Fe_2O_3 (a) and molecularly imprinted polymer modified iron oxide nanoparticles (b). TEM showed particles with rock-like shapes with an average particle diameter (d_0) of 11 nm and a polydispersity σ of 0.36.

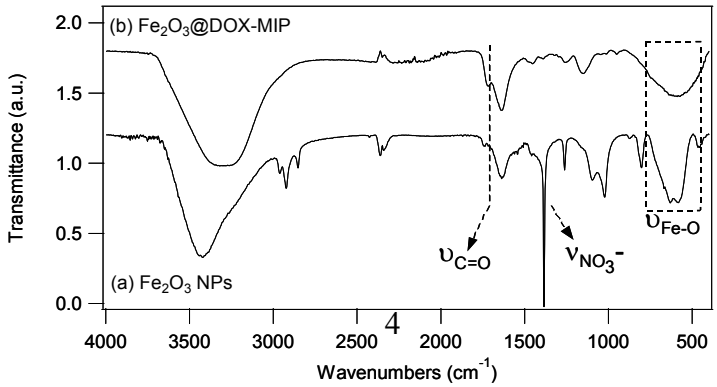

Figure S2. FT-IR spectra of bare Fe_2O_3 (a) and Fe_2O_3@DOX-MIP (b) nanoparticles. The vibration band at 1728 cm^{-1} (C=O stretching) appears when magnetic nanoparticles were covered with MIP that contains a large number of C=O groups in poly-(acrylamide) units confirming the successful growth of polymer.

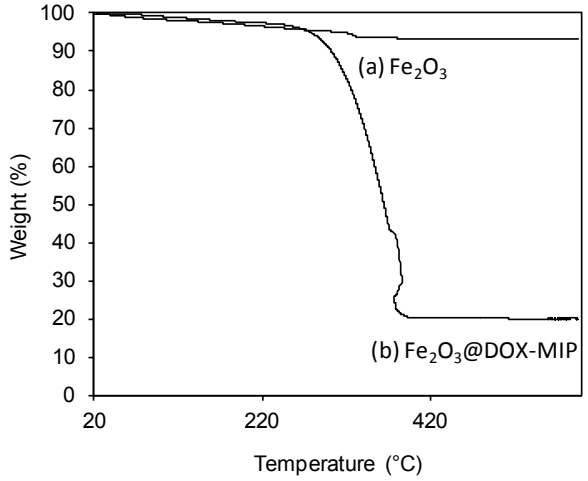

Figure S3. Thermogravimetric analysis of Fe_2O_3(a) and Fe_2O_3@DOX-MIP (b) nanoparticles showing that the amount of MIP on Fe_2O_3@DOX-MIP was about 70% of the total particle weight. During Fe_2O_3@DOX-MIP measurement, an artifact appeared at 370°C but it has no effect on the result.

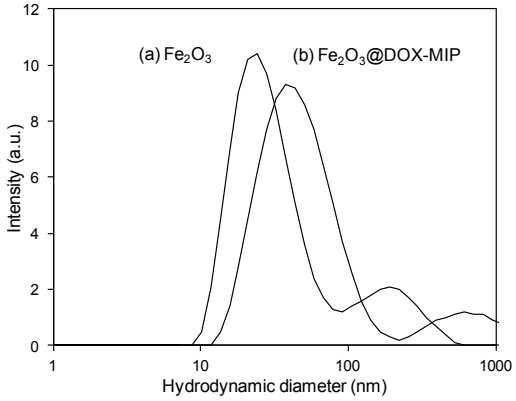

Figure S4. Size distribution from DLS. The Fe_2O_3 NPs were found to be covered with MIP after polymerization as observed by the increase diameter (from 31 to 57 nm).

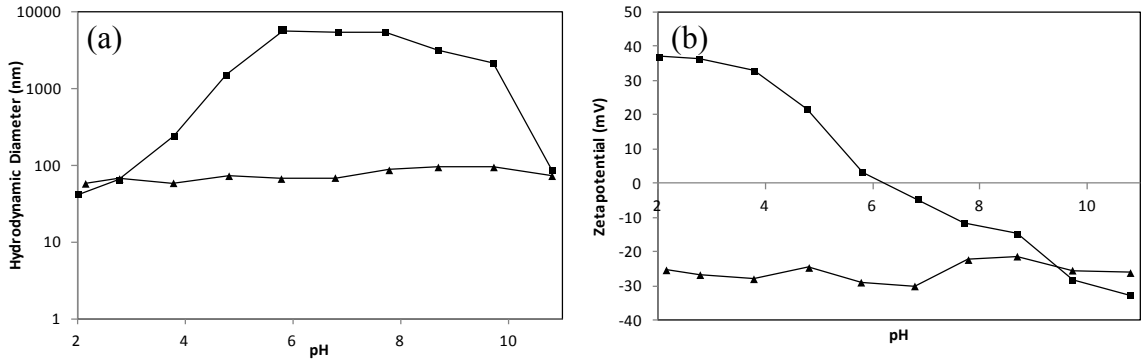

Figure S5. Hydrodynamic diameters (a) and Zeta potential (b) at different pH for bare Fe_2O_3 (square) and Fe_2O_3@DOX-MIP (triangle). Each point corresponds to the average of two experiments.

Sample	d_0 TEM (nm)	sigma	d_0 Mag (nm)	sigma	dh (nm)	pdi	SLP (W/g)
Fe_2O_3	11	0.31	8.4	0.38	31	0.26	97
Fe_2O_3@DOX-MIP	13	0.42	9.5	0.41	57	0.33	67

Table S1. Size distribution (diameter and polydispersity) of Fe_2O_3 and Fe_2O_3@DOX-MIP nanoparticles. d_0 TEM, d_0 Mag and d_h are respectively the mean diameter of the nanoparticles obtained by TEM, by magnetic measurement (VSM) and by DLS.

Adsorption tests

Kinetic adsorption tests. In all experiments, the mass of Fe_2O_3@MIP or Fe_2O_3@NIP was 20 mg, the volume of the adsorption solution was 5 mL, NPs were separated using an external magnet after adsorption, and the amount of free DOX was measured using UV-vis spectrophotometry.

A calibration curve of DOX was performed from the UV absorbance in water at λ_{max} = 485 nm (molar absorption coefficient: 26973 L mol^{-1} cm^{-1})

The adsorption capacity (Q) of the DOX bound to the polymers is defined as:

$$Q = (C_0 - C_s) \times V/m$$

where C_0 and Cs (µM) are the initial concentration and the free analytical concentration in the supernatant of the template DOX, V (L) is the volume of the initial solution, and m (g) is the mass of the NPs.

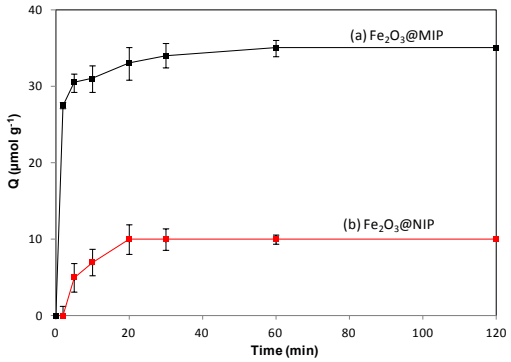

Figure S6. Dynamic rebinding curves of doxorubicin (C_{DOX} = 400µM) on Fe_2O_3@MIPs nanoparticles (black) and Fe_2O_3@NIPs (red) nanoparticles.

Isothermal adsorption experiments

Isothermal adsorption experiments were carried out through varying the concentrations of DOX from 20 to 400 µM during 3 hours. It was shown that the Q of DOX onto the Fe_2O_3@MIP and Fe_2O_3@NIP came to equilibrium over 200 µM.

Scatchard equation

The dissociation constant K_d and Q_{max} can be determined from the slope and intercept of lines obtained by least-squares regression of linear regions of the corresponding Scatchard plots. Here, the data of the static adsorption experiment was further processed with the Scatchard equation as follows:

$$\frac{Q}{[DOX]_{eq}} = \frac{Q_{max} - Q}{K_d}$$

where $[DOX]_{eq}$ is the free template DOX concentration in the solution.

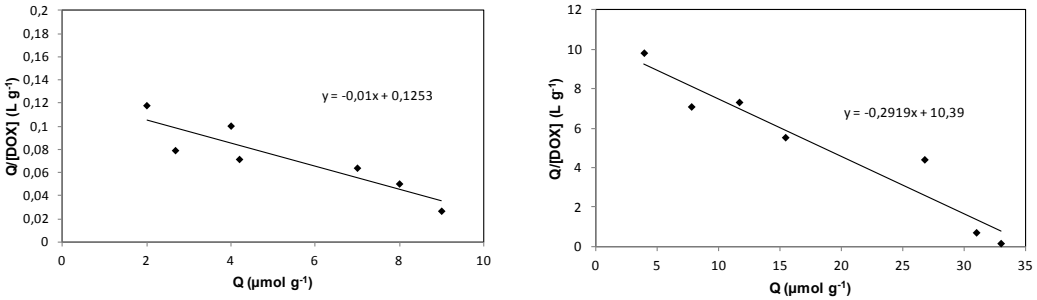

Figure S7. Scatchard plot for the binding of DOX. The dissociation constant K_d and the specific site capacity (Qmax) were calculated from the Scatchard equation. The respective K_d and Q_{max} values are 35.6 µmol g^{-1} and 3.4µM for the Fe_2O_3@DOX-MIP (a) and 12.5µmol g^{-1} and 100µM for the Fe_2O_3@DOX-NIP (b). The difference in DOX binding affinity to the MIP and NIP clearly indicated the role of the imprinting process in the formation of specific binding sites.

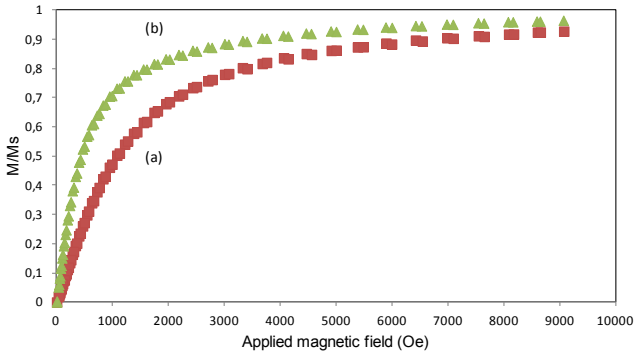

Figure S8. Magnetization curves obtained by vibrating sample magnetometer at room temperature: Fe_2O_3(a) and Fe_2O_3@DOX-MIP (b) nanoparticles.

Release studies

In vitro Fluoresceine, Rhodamine and doxorubicin release studies

In vitro fluoresceine, rhodamine and doxorubicin release studies were monitored in various conditions: in a water bath at human body temperature (37°C) and under an alternative magnetic field (five AMF pulses of 2 minutes with a 30s interval, 335 kHz, 9mT) at 37°C.

For hyperthermia studies, 2 mL of Fe_2O_3@template-MIP, with rhodamine, fluoresceine and doxorubicin as template, in water ([Fe]=0.05 M) was placed at 37°C and submitted to AMF. At each time point the supernatant was collected by magnetic separation and UV/Vis spectroscopy was used to confirm the successful cleavage of the molecule from the MIP and to quantify the amount of molecule released. After the analysis, the supernatant was replaced in the initial eppendorf containing the Fe_2O_3@template-MIP nanoparticles at 37°C for the next measure.

The same protocol was used for Fe_2O_3@template-MIP sample at 37°C but without application of the alternative magnetic field.

Imprinting process role in the DOX release

To compare the drug release experiments, the DOX concentration in the polymer has to be equivalent in the MIP and the NIP. As shown in Figure 1 representing the adsorption isotherms, Fe_2O_3@NIP NPs adsorb the DOX three times lower than the Fe_2O_3@ MIP NPs. Therefore, the Fe_2O_3@NIP NPs are incubated during 4h with 40µM of DOX that is approximatively three times the DOX concentration inside the MIP (12µM). The particles are dialyzed during 24h and washed several times by magnetic separation and finally dispersed in water.

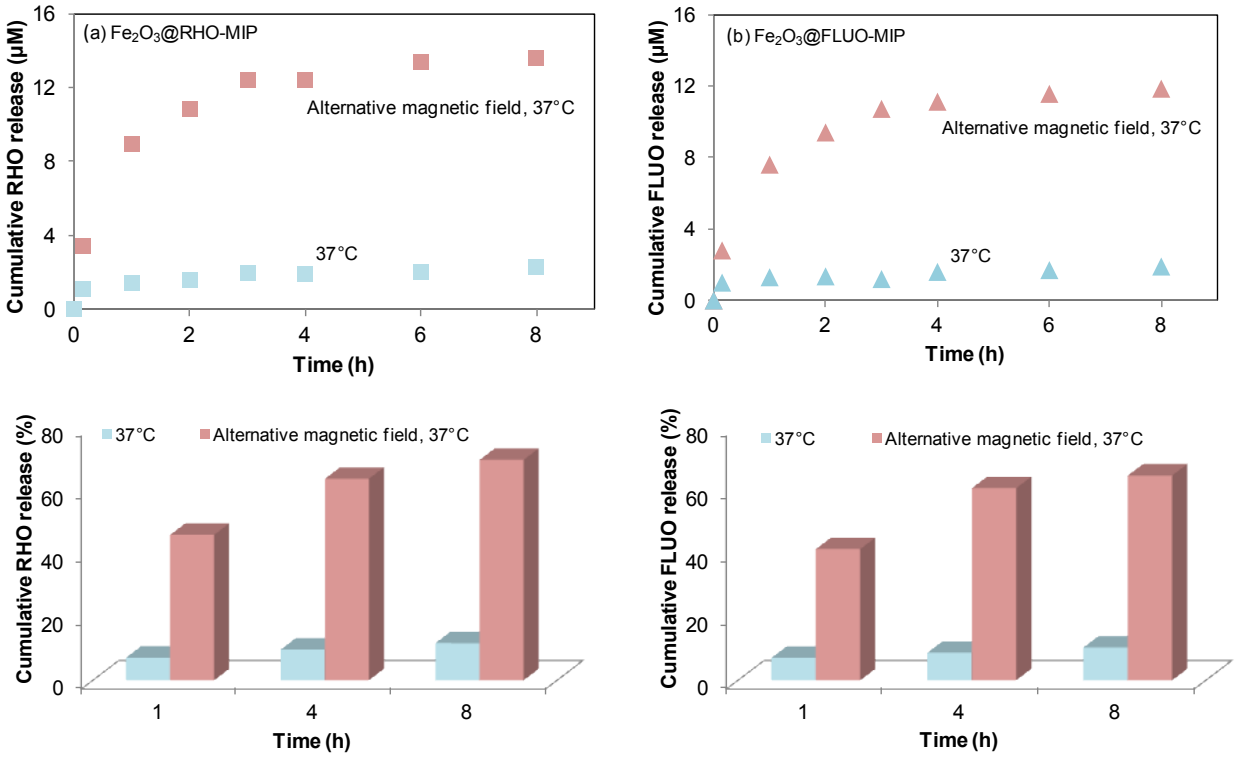

Figure S9. Cumulative DOX release in µmol/L and in percent versus time of (a) Fe_2O_3@RHO-MIP and (b) Fe_2O_3@FLUO-MIP nanoparticles ([Fe]=50 mM) at 37°C without magnetic field and under AMF (335 kHz, 9mT).

To determine the concentration of DOX inside the MIP, a calibration curve was done by submitting 2 mL of Fe_2O_3@DOX-MIP NPs in water ([Fe]=0.05 M) to a mixture of ethanol/acetic acid (9:1v/v) in order to extract the DOX from the MIP. After 10 min, the supernatant was collected by magnetic separation and the amount of DOX was measured by UV/Vis spectroscopy. After the analysis, the supernatant was replaced in the initial eppendorf containing the Fe_2O_3@DOX-MIP nanoparticles at room temperature. The same supernatant was then analyzed after 1, 2, 3, 4, 6 and 8h.

Effect of the magnetic core on the drug release process

To show the crucial role of the Fe_2O_3 NPs in the drug release process, DOX was first extracted from the polymer (2mL, [Fe]=0.05 M) with a mixture of ethanol/acetic acid (9:1v/v). Then the magnetic core was dissolved in HCl (37%), and after separation of the

polymer from the acidic solution by ultracentrifugation, the MIP was incubated with DOX (40µM) during 3hours. The excess of DOX was removed by several ultracentrifugation steps until no DOX was detected by UV/Vis spectroscopy in the solution containing the polymer. In vitro DOX release studies were then monitored at 37°C under AMF after 1, 2, 3, 4, 6 and 8h on the same sample. The supernatant collected by ultracentrifugation was analyzed by UV/Vis spectroscopy.

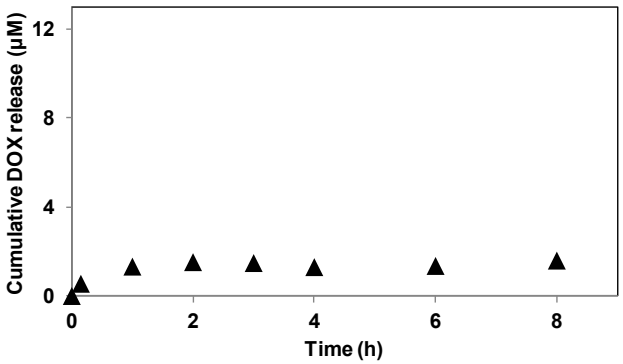

Figure S10. Cumulative DOX release in µmol/L versus time of DOX-MIP at 37°C under alternative magnetic field (335 kHz, 9mT).

Effect of the temperature on the DOX release

Fe_2O_3@DOX-MIP (2mL, [Fe]=0.05 M) nanoparticles (5 samples) were submitted to water bath at different temperatures (24, 37, 50, 70 and 85°C) during 4 hours. After 4 hours, the supernatant was collected by magnetic separation and UV/Vis spectroscopy was used to confirm the successful cleavage of DOX from the MIP and to quantify the amount of DOX release.

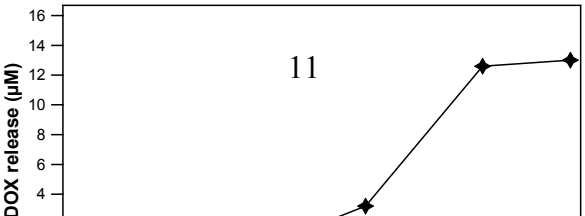

Figure S11. Influence of the temperature (water bath) on the amount of DOX released from Fe_2O_3@DOX-MIP nanoparticles ([Fe]=50 mM).

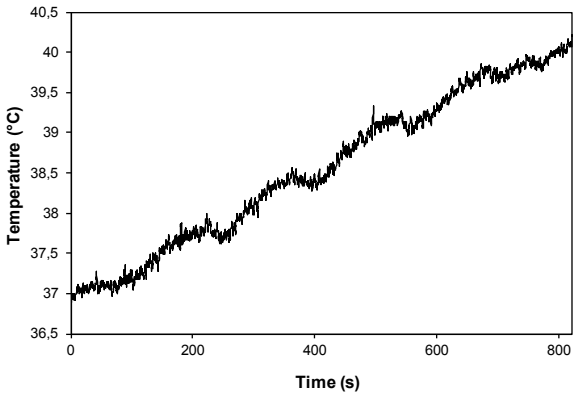

Figure S12. Temperature variation of Fe_2O_3@DOX-MIP in water (2 mL, [Fe]=0.05 M)) after 5 cycles of 2 min excitation at 335 kHz, 9 mT, and 30s without excitation. The temperature of the magneTherm measurement cell was 40°C after the AMF exposure

Living cells experiment

Human Prostatic Cancer Cell lines (PC-3, ATCC® CRL-1435™) were cultured at 37°C in 5% CO_2 in Dulbecco's modified Eagle's medium (DMEM) completed with 10% fetal bovine serum and 1% penicillin and streptomycin antibiotics. Fe_2O_3@DOX-MIP NPs were incubated with the cells for 2 hours at iron concentrations in the range [Fe]=0.5-2 mM. Control Fe_2O_3@citrate NPs (same iron oxide core with simple citrate coating) were incubated for the

same 2h time period, at [Fe]=2 mM. Incubation was followed by an overnight chasing period in complete medium.

Cellular iron load was measured by single-cell magnetophoresis (Figure S13). Briefly, after incubation cells were detached and suspended in a chamber subjected to a calibrated magnetic field gradient (17 T/m) created by a permanent magnet. Single cells migration towards the magnet was video-monitored and cell diameters (d_{cell}) and velocities (v_{cell}) were measured. The magnetisation per cell (M_{cell}) was then computed for 200 independent cells by balancing the magnetic force (M_{cell}gradB) with the viscous drag ($3\pi\eta d_{cell}v_{cell}$, η being the water viscosity). The mass of iron per cell is then proportional to Mcell (for the maghemite nanoparticles used here, a magnetic moment of $6.6x10^{-14}$ Am² corresponds to 1 pg of iron).

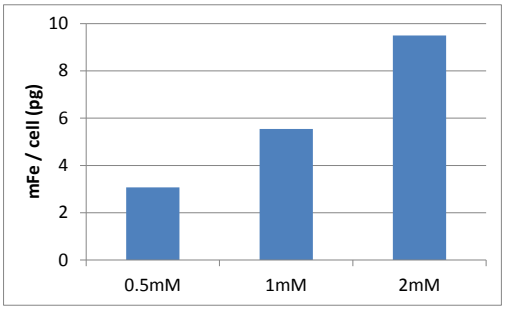

Figure S13. Iron load per cell after a 2-hours incubation with Fe_2O_3@DOX-MIP at [Fe]=0.5-1-2 mM.

For confocal microscopy observation (Figure S14), cells membranes were then labeled by PKH26 red dye, cells were fixed right after with 2% paraformaldehyde, and in some cases poststained with DAPI (4',6-diamidino-2-phenylindole) to localize the nucleus.

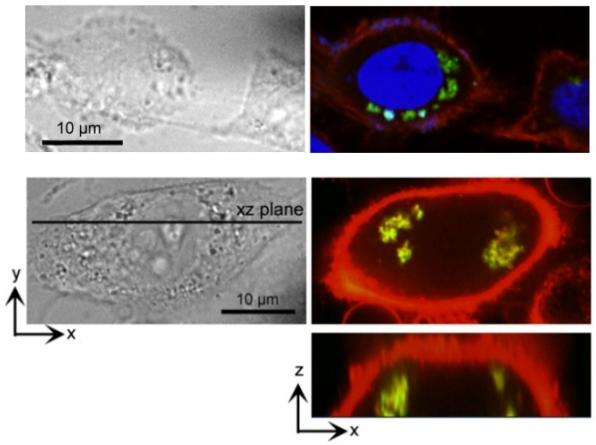

Figure S14. Confocal imaging of tumour cells having internalized Fe_2O_3@DOX-MIP nanoparticles (2-hours incubation at [Fe]=2 mM). DOX is detected in the green channel (excitation at 488 nm, emission at 561 nm). Nuclei and cell membranes are stained by DAPI in blue (top image) and PKH26 in red, respectively. Z reconstructions (bottom) identify DOX inside the cells. Bright field images are shown on the left.

For AMF-induced doxorubicin release in the cellular environment, cells were exposed to the alternative magnetic field (thermostated at 37°C) for 30 min, 1h30, and 2h30. The AMF treatment recorded no macroscopic heating (Figure S15). Viability measurements were performed the day after using Alamar blue colorimetric assay.

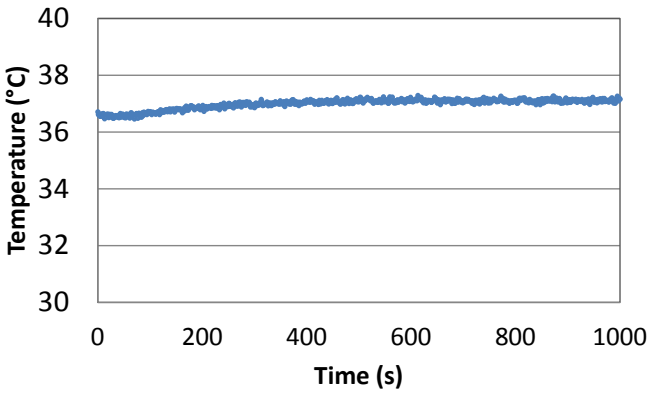

Figure S15. Temperature increase (from 36.5 to 37°C) during AMF exposure with cells, corresponding to athermal conditions.